Bimonthly Report No. 2

March 3, 1963 to May 2, 1963

5549-2-P

STUDY AND INVESTIGATION OF A UHF-VHF ANTENNA

by

A. T. Adams
R. M. Kalafus

5549-2-P = RL-2126

Approved by John A M Lyon by B A Barton
John A. M. Lyon

COOLEY ELECTRONICS LABORATORY

Department of Electrical Engineering
The University of Michigan
Ann Arbor

United States Air Force
Air Force Systems Command
Aeronautical Systems Division
Contract No. AF 33(657)-10607
Wright-Patterson Air Force Base, Ohio

June 1963

MISSING PAGE

TABLE OF CONTENTS

LIST OF ILLUSTRATIONS

LIST OF ILLUSTRATIONS (Cont.)

ABSTRACT

Data on the aperture admittance of a loaded rectangular waveguide antenna are given and compared with experimental results. Theoretical efficiency data for a loaded rectangular cavity slot antenna is compared with experimental data. With powdered ferrite material presently available, efficiency is 65 percent. With solid ferrite material presently available, theoretical results predict 20 percent efficiency.

1. REPORTS, TRAVEL, AND VISITORS

During this period no reports were issued, no travel undertaken, and no one visited the project.

2. FACTUAL DATA

2.1 Rectangular Cavity Variational Results

A stationary expression for the normalized aperture admittance of a loaded waveguide radiator (Fig. 1) was formulated in QPR No. 9 (formula 8, p. 17). The expression was then expanded into the form shown on page 28 of QPR No. 9, the first term of which represents the dominant mode approximation to the aperture field.

Dominant Mode Approximation:

$$\frac{Y}{Y_o} = G + jB$$

$$= -\frac{4\mu_r}{\Gamma_{10} ab} \int_0^a \int_0^b (b-\sigma) \left| (a-\lambda)\left(k_o^2 - \frac{\pi^2}{a^2}\right) \cos\frac{\pi\lambda}{a} \right.$$

$$\left. + \frac{a}{\pi}\left(k_o^2 + \frac{\pi^2}{a^2}\right) \sin\frac{\pi\lambda}{a} \right| \frac{e^{-jk_o\sqrt{\lambda^2+\sigma^2}}}{2\pi\sqrt{\lambda^2+\sigma^2}} \, d\sigma \, d\lambda$$

MISSING PAGE

where:

μ_r = relative permeability of loading material

k = material wave number (ka = π at cutoff)

k_o = free space wave number

This double integral has been evaluated using the IBM 7090 computer. Preliminary data were presented in BMR No. 2 which covered the period January 3, 1963, to March 2, 1963. Since then, more extensive data has been obtained and is presented in Fig. 2. The data is sufficiently extensive to allow accurate interpolation for intermediate values of b/a, $\mu\epsilon$ and frequency.

For all the data presented, μ_r is equal to ϵ_r. However, each figure with a given μ_r and ϵ_r may be expanded to give a family of figures for the same $\mu_r \epsilon_r$ product but different μ_r / ϵ_r ratios. This additional data is obtained by multiplying the real and imaginary parts of the admittance by $\frac{\mu_r \text{ (actual)}}{\mu_r \text{ (figure)}}$. For instance, Fig. 2(e) can be converted to ($\mu_r = 4.5$, $\epsilon_r = 2$) by multiplying B and G by $\frac{4.5}{3.0}$.

Formulas for Large $\mu_r \epsilon_r$:

For $\mu_r \epsilon_r$ products greater than 100, the following approximate formulas apply:

$$G = \frac{2\mu_r (k_o^2 a^2 - \pi^2)}{\pi^3 \sqrt{k^2 a^2 - \pi^2}} \left\{ (k_o b)(c+1) - \frac{(k_o b)^3}{36\pi^2} \left[(c+1)\pi^2 + \frac{3a^2}{b^2} \left[(\pi^2 - 4)(c+3) - 2\pi^2 \right] \right] \right\}$$

$$\approx \frac{4}{k^2 a^2 - \pi^2} \left(\frac{ka}{\pi}\right)^3 \frac{b}{a} \frac{1}{(\mu_r)^{1/2} (\epsilon_r)^{3/2}}$$

MISSING PAGE

MISSING PAGE

MISSING PAGE

MISSING PAGE

MISSING PAGE

MISSING PAGE

MISSING PAGE

MISSING PAGE

MISSING PAGE

MISSING PAGE

where:

$$C = \frac{k_o^2 a^2 - \pi^2}{k_o^2 a^2 - \pi^2}$$

$$B \approx -\frac{2}{\pi} \frac{\mu_r}{\sqrt{k^2 a^2 - \pi^2}} F_1(\theta_1)$$

where:

$$\theta_1 = \tan^{-1} b/a$$

$$F_1(\theta_1) = 4 \log \tan\left(\frac{\theta_1}{2} + \frac{\pi}{4}\right) - \frac{a}{b}(\sec\theta_1 - 1)$$

$$+ \int_{\theta_1}^{\pi/2} \frac{a}{b} \tan\theta \sec\theta \left[1 - \cos\left(\frac{\pi b \operatorname{ctn}\theta}{a}\right)\right] d\theta$$

$$+ \int_{\theta_1}^{\pi/2} \sec\theta \left[\cos\left(\frac{\pi b \operatorname{ctn}\theta}{a}\right) - \frac{a}{b\pi} \tan\theta \sin\left(\frac{\pi b \operatorname{ctn}\theta}{a}\right)\right] d\theta$$

$$+ \int_{\theta_1}^{\pi/2} 2 \sec\theta \left[1 - \cos\left(\frac{\pi b \operatorname{ctn}\theta}{a}\right)\right] d\theta$$

$$\frac{B}{G} \approx -\frac{1}{2\pi}\left(\frac{a}{b}\right) \frac{(\mu_r)^{3/2} (\epsilon_r)^{3/2}}{\left(\frac{ka}{\pi}\right)^3} F_1(\theta_1)$$

The above formulas were derived by assuming small angle approximations. for $\sin(k_o \sqrt{\lambda^2 + \sigma^2})$ and $\cos(k_o \sqrt{\lambda^2 + \sigma^2})$.

2.2 Experimental Verification of Variational Data

An experimental check on the variational data was carried out, using Emerson and Cumming Stycast Hi-K with characteristics ($\mu_r = 1$, $\epsilon_r = 10$). Equipment used in the experiment is shown in Figs. 3 and 4. The 2' x 3' ground plane shown in Fig. 3 was mounted in the ground plane at the end of the Anechoic chamber at the countermeasures laboratory. At the frequencies checked (2 - 4 kMc), the Anechoic chamber has very good characteristics. A sketch of the experimental arrangement is shown in Fig. 5. Light absorbing pads were mounted around the 2' x 3' ground plane to simulate as nearly as possible an infinite ground plane. Impedance was obtained by conventional slotted-line methods using an X-band slotted line.

The geometry of the slotted dielectric insert is shown in Fig. 6. Because of the slot, the geometry differs from the theoretical model. Tapered dielectric wedges were also used (Fig. 4). Impedance was measured both with and without the wedges inserted. The wedges were used to provide a measurement of the impedance of a geometry corresponding to the theoretical calculations. For the data measured, the impedance falls in a portion of the Smith chart where the constant G curves are very nearly parallel to the constant VSWR circles. Thus G can be determined by the magnitude of the reflection coefficient alone.

MISSING PAGE

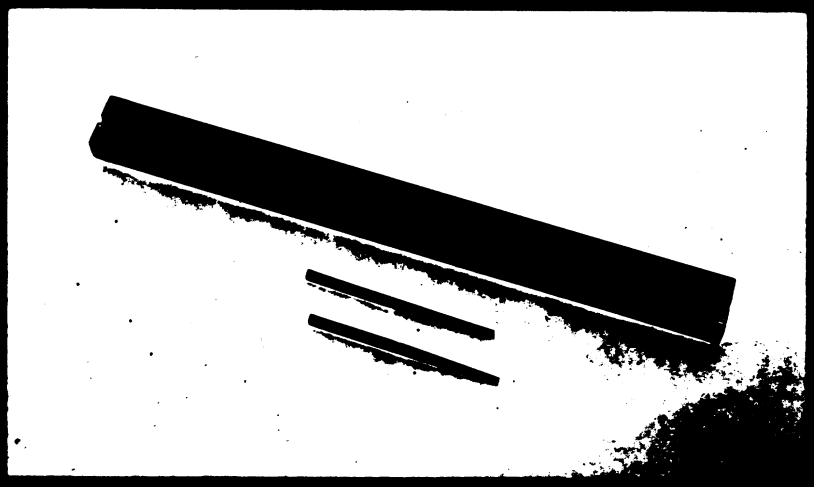

Fig. 4. Slotted dielectric and wedges.

MISSING PAGE

The taper constitutes a gradual transformation from the rectangular dielectric cross section to the slotted dielectric cross section and introduces little reflection at frequencies where the taper length is appreciable compared to the guide wavelength. Near cutoff, the reflection introduced by the taper may become significant. Thus, at frequencies slightly above cutoff, the VSWR and G measured should correspond to that of the theoretical model. The value of B depends on the transformation through the wedged section. Since the electrical length of the wedged section is taken into account by a measurement of minimum position with a short on the waveguide, it would be expected that a minimum position measurement without the short would give an accurate measurement of the angle of the aperture reflection coefficient. The data without wedge represents an accurate measurement of the impedance of a geometry differing from the theoretical model. The data with the wedge represents a less accurate measurement of the impedance of a geometry identical to the theoretical model, with accuracy increasing as frequency increases.

The presence of the slot in the dielectric modifies the cutoff wavelength as well as the equivalent circuit of the discontinuity. Unfortunately, the effect of the slot cannot be taken into account by perturbation formulas. The boundary conditions on E_x at the sides of the slot (surface A of Fig. 6) require continuity of E_x, while the

boundary conditions at the bottom of the slot (surface B of Fig. 6) require continuity of ϵE_x. According to perturbation formulas, these two conditions would tend to change λ_g in different directions. Thus the change in λ_g due to the slot is not readily predictable from boundary conditions. However, we know that guide wavelength has the form:

$$\lambda_g = \frac{\lambda_o}{\sqrt{\epsilon_{eff}}} \cdot \frac{1}{\sqrt{1 - (f_c / f)^2}}$$

where: ϵ_{eff} = effective dielectric constant of the dielectric-guide and air-slot configuration. Two measurements of guide wavelength determine the two unknowns ϵ_{eff} and f_c.

Let

$$\left(\frac{\lambda_{o1}}{\lambda_{g1}}\right)^2 \Big/ \left(\frac{\lambda_{o2}}{\lambda_{g2}}\right)^2 = A$$

Then

$$f_c = \frac{1 - A}{\frac{1}{f_1^2} - \frac{A}{f_2^2}}$$

Using this method, f_c was calculated using several measurements of guide wavelength. The values varied from 2130 to 2177 Mc with an average of 2160 Mc. This value was used in plotting F_N (Figs. 7(a) and (b)). The theoretical value for cutoff of a waveguide completely filled with dielectric material of dielectric constant 10 is 2080 Mc.

MISSING PAGE

MISSING PAGE

Figures 7(a) and 7 (b) show the results of the experimental check. The experimental and theoretical values of B show good agreement. the experimental data with wedge falling very close to the theoretical values. The results for G also appear to be accurate, although it is somewhat more difficult to obtain an accurate comparison. The experimental data shown in Figure 7(b) is slotted assuming a lossless sample. If the attenuation is taken into account (by a measurement with the sample shorted), the experimental data approaches the theoretical data. However, some refinements in technique are necessary to ensure accurate attenuation measurements.

Further tests will be carried out for values of ϵ_r of 4 and 16.

2.3 Efficiency of Ferrite Loaded Slot Antennas

The efficiency of a loaded rectangular cavity slot antenna was analyzed in BMR No. 1. Using the analysis for one of the simpler cases (probe near aperture, low losses, magnetic losses only), theoretical data for efficiency was calculated and compared with experiment.

From BMR No. 1 (page 27)

Magnetic volume losses only

$$\text{Efficiency} = \frac{1}{1 + \frac{\bar{P}_L}{\bar{P}_R}}$$

$$\frac{\bar{P}_L}{\bar{P}_R} = \left(\frac{\mu''}{\mu'}\right)\left[k^2 a^2 \left(\frac{2d}{a}\right) + \frac{(k^2 a^2 - 2\pi^2)\sin 2\beta_{10} d}{\sqrt{k^2 a^2 - \pi^2}}\right] \Big/ (1 - |R|^2)\sqrt{k^2 a^2 - \pi^2}$$

where d = length of cavity

R = complex aperture reflection coefficient

$$\beta_{10} = \frac{\sqrt{k^2 a^2 - \pi^2}}{a}$$

Using the above formula, theoretical efficiency data was calculated for two cases, $\mu = \epsilon = 3$ and $\mu = \epsilon = 10$. d was calculated using theoretical aperture admittance data (BMR No. 1 Table No. II). Figure 8 shows μ''/μ' data for the ferrite powder material used in the experiments.

MISSING PAGE

Figure 9 shows theoretical and experimental data for the ferrite powder loaded rectangular cavity antenna. Figure 10 shows theoretical data only for $\mu = \epsilon = 10$, using the same μ''/μ' data.

The efficiency was measured using reflection techniques as described in QPR No. 10 and Ref. 1. The tests were made in the anechoic chamber of the countermeasures laboratory. The rectangular cavity slot antennas was mounted in the large ground plane at one end of the anechoic chamber. Four aluminum "hats" of different sizes were alternately placed over the antenna and bolted to the ground plane. The impedance measurements with the four hats lie on a circle on the Smith chart. The efficiency, as defined in Ref. 1 , is equal to

$$\frac{2 D_1 D_2}{(D_1 + D_2)(1 - D_3^2 / R^2)}$$

where D_1 = longest distance from Z_a to the edge of the circle.

D_2 = shortest distance from Z_a to the edge of the circle.

D_3 = distance from Z_a to center of the Smith chart.

R = radius of the Smith chart.

Z_a = impedance of the antenna in free space.

For the measurement of Z_a, light lossy pads were placed on the ground plane and a large (10' x 10') array of lossy pyramids was placed in front of the antenna in order to reduce reflections as much as possible. Smith chart plots are shown in Fig. 11. Efficiency is calculated directly

MISSING PAGE

MISSING PAGE

from the plots and then corrected taking into account cable losses. Efficiency measurements were taken at 315 Mc and 227 Mc.

The results for this simple theoretical model show good agreement between theory and experiment. The low frequency case (227 Mc) shows a greater discrepancy than the high frequency case (315 Mc). However, the experimental data for 227 Mc is less reliable, as is indicated by Fig. 11 (C).

The theoretical data of Fig. 10 indicates efficiencies of about 20 percent for a solid ferrite material. Experiments with a solid ferrite antenna are underway, and efficiency measurements will be made for a further check on the theory.

MISSING PAGE

MISSING PAGE

MISSING PAGE

3. ACTIVITIES FOR THE NEXT PERIOD

Two graduate students have been added to the project to aid in an investigation of loaded traveling wave antennas. Emphasis will be placed upon the spiral and the log conical antennas. Further checks will be made on the theoretical variational data shown in this report. Impedance and efficiency characteristics of solid ferrite loaded and dielectric loaded rectangular cavity antennas will be investigated.

4. SUMMARY

Extensive data on the aperture admittance of a loaded rectangular waveguide radiator is given. An experimental check shows good agreement between theory and experiment. This basic data is used in calculations of bandwidth, resonant frequency, and efficiency. Theoretical and experimental values of bandwidth and resonant frequency have been compared in previous reports. Theoretical and experimental values of efficiency are compared in this report. Agreement between theory and experiment is good, showing promise for design methods based on this combination of variational techniques and Smith chart calculations.

REFERENCES

1. Interim Engineering Report on Miniature, Zero-Drag, Broadband, Tunable Cavity Antennas, 1 July to September 1953, University of Oklahoma Research Institute, Contract No. AF 33(038)-10405.